DNA Prime-Protein Boost Targeting Conformational Non-RBD Region for Broad Cross-Neutralization

Yun-Fei Ma[1, #], Kun Chen[2, #], Bowen Xie[1, #], Jiayi Zhu[2, #], Xuan He[3, 4], Chunying Chen[2, *], Yuhe Renee Yang[2, *], Ye Liu[1, 5, 6 *]

[1]Institute of Medical Biology, Chinese Academy of Medical Sciences and Peking Union Medical College, Kunming, Yunnan 650000, China.

[2]CAS Key Laboratory of Nanosystem and Hierarchical Fabrication, CAS Center for Excellence in Nanoscience, National Center for Nanoscience and Technology, Beijing 100190, China.University of Chinese Academy of Sciences, Beijing 100049, China

[3]Department of Respiratory and Critical Care Medicine, Frontiers Science Center for Disease-Related Molecular Network, West China Hospital, Sichuan University, Chengdu 610213, China.

[4]Precision Medicine Research Center, West China Hospital, Sichuan University, Chengdu 610041, China.

[5]State Key Laboratory of Respiratory Health and Multimorbidity, Beijing, 100190 (P. R. China)

[6]Key Laboratory of Pathogen Infection Prevention and Control (Peking Union Medical College), Ministry of Education, Beijing, 100190 (P. R. China)

[#]These authors contributed equally

*e-mail: liuye@imbcams.com.cn; yangyh@nanoctr.cn; chenchy@nanoctr.cn

SUMMARY

The preservation of antigen spatial conformation is crucial for inducing the high-quality neutralizing responses. Although the receptor-binding domain (RBD) antigen in SARS-CoV-2 vaccines shows satisfactory conformation preservation, it remains susceptible to the immune escape. Therefore, exploring conformational epitopes beyond the RBD region to achieve cross-neutralization becomes an attractive topic. In this study, we used a DNA prime-protein boost regimen to obtain potent humoral responses. Further analysis revealed that boosting antibody responses targeting conformational non-RBD region is crucial for enhancing cross-neutralization against the Wuhan-01, Delta and Omicron subvariants. *Via* analyzing the distribution of conformational epitopes, and quantifying epitope-specific binding antibodies, we verified a positive correlation between the proportion of binding antibodies against the N-terminal domain (NTD) supersite (a conformational non-RBD epitope) and SARS-CoV-2 neutralization potency. The current work highlights the importance of conformational non-RBD-specific binding antibodies in mediating viral cross-neutralization and provides a new insight in overcoming the immune escape of SARS-CoV-2 variants.

INTRODUCTION

Preserving the spatial conformation of antigens is critical for effectively inducing neutralizing antibody responses (Impagliazzo et al., 2015; Sesterhenn et al., 2020; Xu et al., 2022). For SARS-CoV-2 vaccines, although the RBD as core antigen can preserve a satisfactory spatial conformation (Dai et al., 2022; Xu et al., 2022; Yang et al., 2023a), RBD antigen suffers a continuous emergence of new variants, which is easy to result in a marked decline in the protection efficacy (Cox et al., 2023; Gu et al., 2020; Huang et al., 2022; Huang et al., 2023). In contrast, non-RBD region mutates at a lower and slower frequency (Chi et al., 2020; Liu et al., 2020; Wang et al., 2022), suggesting a more promising potential in limiting the immune escape from viral variants. However, up to now, there is still few successful reports *via* constructing conformational non-RBD region-based vaccines to induce potent neutralizing antibodies. One important reason is how to preserve the spatial conformation of epitopes in non-RBD region still suffers a big challenge (Vishweshwaraiah et al., 2022; Voss et al., 2021).

The non-RBD region is divided into two discontinuous fragments by RBD domain (Gobeil et al., 2021). If non-RBD antigens are harvested *via* fragment-fusion or fragment-separated expression *in vitro*, the spatial conformation of epitopes in non-RBD region would be very possibly undergo a significant change (Olmedillas et al., 2023) (details showed in Figure 1 in results section). Therefore, it is very challenging to obtain conformational non-RBD antigen by the traditional protein expression strategy. To address this challenge, we selected two distinct approaches. One is 'full-length S prime and RBD boost' (S prime-RBD boost), which only boosts the conformational RBD-specific antibodies. The other is 'full-length S prime and full-length S boost' (S prime-S boost), which can boost both conformational non-RBD- and RBD-specific antibodies. *Via* comparing the difference of antibody profile between 'S prime-RBD boost' and 'S prime-S boost', we can understand the roles of conformational non-RBD in mediating the neutralizing antibody responses.

In the current study, we found that boosting conformational non-RBD region can significantly enhance cross-neutralization against SARS-CoV-2 strains. Furthermore, by a combined analysis of intelligentized epitope identification and electron

microsocopy (EM) techniques, we identified NTD supersite (McCallum et al., 2021; Wang et al., 2022) as a critical conformational epitope in non-RBD region in contributing to increase SARS-CoV-2 cross-neutralization. This finding shed light on the underlying mechanism of conformational non-RBD epitopes in mediating cross-neutralizing SARS-CoV-2 variants.

RESULTS

Analyzing the conformational epitopes in RBD and non-RBD region.

Preserving the spatial conformation of vaccine antigens is critical for effectively inducing neutralizing antibodies against SARS-CoV-2 strains (Cao et al., 2023; Dai et al., 2020). In the current study, we used the conformation similarity as the index to analyze the preservation of conformational epitopes in the full-length S antigen. Most of the published crystal structure of *in vitro*-expressed full-length S protein is closely similar (< 3 Å) with the structure of the original viral S protein (Bangaru et al., 2020; Cai et al., 2020). We therefore quantified the conformation similarity based on the root mean square deviation (RMSD) value *via* comparing the overlap ratio between the spatial conformation of non-RBD/RBD antigens and the spatial conformation of full-length S antigen (control). According to the published studies, the RMSD value which is more than 3 Å represents a significant difference in epitope conformation (Gainza et al., 2023; Sesterhenn et al., 2020).

In the full-length S protein, the amino acid sequence of non-RBD region is separated into two parts by RBD region which possesses a coherent amino acid sequence. For the design of conformational non-RBD antigens, in general, two separated non-RBD parts would be either directly pieced into a whole (w/o linker) or jointed together with a linker (with linker) (Chen et al., 2013; Lu et al., 2022) (Figure 1A). We calculated the RMSD value of non-RBD (w/o linker) and non-RBD (with linker) antigen for 18 SARS-CoV-2 strains (Table S1). The $RMSD_{\text{non-RBD (w/o linker)}}$ and $RMSD_{\text{non-RBD (with linker)}}$ is ranged from 4.0 to 13.1 Å and 3.9 to14.3 Å, which are more than 3 Å (Figures 1B-1K and S1). This result showed that *in vitro*-expressed non-RBD antigen hardly preserves its spatial conformation. In contrast, the RMSD value of RBD

antigen is ranged from 0.5 to 1.6 Å (< 3 Å, Figures 1B-1K and S1), indicating that *in vitro*-expressed RBD antigen can maintains its spatial conformation. Together, the spatial conformation of non-RBD antigen, instead of RBD antigen, is hardly obtained *via in vitro* protein expression. Therefore, injecting non-RBD protein very possibly fail to induce the antibody response against the conformational non-RBD epitopes.

DNA prime-protein boost elicits higher levels immune response in mice than protein alone

To effectively induce the antibody responses against conformational non-RBD epitopes, we selected a 'DNA prime-protein boost' strategy. The plasmid expressed the full-length S antigen is used as prime once. Either the full-length S protein or RBD protein was used as boost twice. After two-round boost, 'S prime-RBD boost' ensure that almost vaccine-induced antibodies are specific to conformational RBD epitopes. However, 'S prime-S boost' would induce abundant antibodies against the conformational epitopes in both RBD and non-RBD region. By the further comparison of antibody profiles between 'S prime-RBD boost' and 'S prime-S boost', we would possibly understand the unrevealed roles of conformational non-RBD epitopes in mediating the neutralizing antibody responses.

Of course, it is still necessary to verify whether 'DNA prime-protein boost' is an effective strategy for the induce of potent antibody responses. To assess the effects of 'DNA prime-protein boost' regimen, we designed the vaccination plan as followings: at the prime stage, BALB/c mice were intramuscularly immunized by a single dose of 15 μg of RBD or S protein-expression plasmid. After two weeks, the mice were intramuscularly immunized with two doses of either RBD or S protein (10 μg per injection) as boost (RBD_{DNA}-RBD-RBD/S_{DNA}-S-S), with a two-week interval between boost injections. As controls, we set up two additional groups in which mice received three immunizations of either RBD or full-length S protein (RBD-RBD-RBD/S-S-S) throughout the entire immunization regimen (Figures 2A and 2E). Serum samples were collected after two weeks of the 2nd boost immunization for the detection of antibody responses.

For the vaccination regimen with RBD protein booster, RBD-specific IgG response in mice receiving DNA prime-RBD protein boost was 2.82-fold higher than that in mice receiving RBD protein alone ($P < 0.05$, Figure 2B). The titer of RBD-specific IgG2a and IgG2b in DNA prime-RBD protein boost vaccinated mice was significantly higher than that in mice receiving RBD protein alone ($P < 0.05$, Figure 2C), and IgG1 and IgG3 in DNA prime-RBD protein boost were not less than those of receiving RBD protein alone. Correspondingly, in the live virus neutralization tests, the mice receiving the DNA prime-RBD protein boost exhibited a 2.16-fold higher neutralizing antibody response against Wuhan-Hu-01 strain ($P < 0.01$, Figure 2D), 3.28-fold higher neutralizing antibody response against B.1.1.529 strain (Omicron) ($P < 0.001$, Figure 2D) and similar strength of neutralizing antibody response against B.1.617.2 strain (Delta) ($P = 0.1717$, Figure 2D), in comparison to the mice receiving RBD protein alone.

Similar results were observed for the vaccination regimen with S protein (non-RBD and RBD epitopes) boost. Compared with mice received S protein alone, mice that received the DNA prime-S protein boost obtained a 1.67-fold higher S-specific IgG response ($P < 0.05$, Figure 2F). S protein-specific IgG2a and IgG2b response in mice that received the DNA prime-S protein boost was also significantly increased ($P < 0.05$) compared to those mice that received S protein alone (Figure 2G). In contrast, S-specific IgG1 and IgG3 response did not show significant difference between the mice vaccinated with DNA prime-S protein boost and the S proteins alone. Furthermore, mice receiving DNA prime-S protein boost exhibited a 2.92-fold higher neutralizing antibody response against the Wuhan-Hu-01 strain ($P < 0.01$, Figure 2H), 2.28-fold higher neutralizing antibody response against the B.1.617.2 strain (Delta) ($P < 0.05$, Figure 2H) and 3.78-fold higher neutralizing antibody response against the B.1.1.529 strain (Omicron) ($P < 0.05$, Figure 2H).

These results showed that, compared with receiving protein alone, DNA prime-protein boost vaccination induced significantly stronger binding antibody and cross-neutralizing antibody response. Taken together, 'DNA prime-protein boost' strategy can dramatically enhance the efficacy of vaccine in inducing humoral responses in the host.

Boosting conformational non-RBD epitopes to improve SARS-CoV-2 cross-neutralizing response.

In order to explore the role of boosting conformational non-RBD epitopes in the cross-neutralizing responses against SARS-CoV-2 strains, we compared the humoral responses in mice receiving the boost vaccination with either RBD protein alone (conformational non-RBD epitopes were not boosted) or full-length S protein (conformational non-RBD epitopes were boosted). At the prime stage, all mice received a single dose of DNA vaccine (15 μg), which expresses full-length S protein. At the boost stage, the mice were divided into two groups. One group received two doses of RBD protein alone (S_{DNA}-RBD-RBD), aiming to only boost RBD-specific humoral responses. Another group received two doses of full-length S protein (S_{DNA}-S-S). Our above-mentioned analysis (Figures 1B-1K and S1) indicated that full-length S protein, instead of *in vitro*-expression non-RBD protein, possesses the consistent conformational epitopes within non-RBD region. Therefore, comparing Group (S_{DNA}-RBD-RBD) and Group (S_{DNA}-S-S) together can provide us with a clearer understanding of the advantages and role of the non-RBD region in mediating immune responses. At the boost stage, the dosage of protein vaccine (RBD or full-length S) is 10 μg for each injection.The interval of boost vaccination is two weeks (Figure 3A). Mouse serum samples were collected after two weeks of the final vaccination for detection of the humoral responses.

The titer of IgG was increased by 23.47-fold in mice receiving a full-length S protein boost (S_{DNA}-S-S), in comparison to those receiving an RBD boost (S_{DNA}-RBD-RBD) (Figure 3B). IgG1, IgG2a, IgG2b and IgG3 response in full-length S protein-boost group was 1.11-fold, 87.47-fold, 87.47-fold and 26.32-fold higher than that in RBD-boost group ($P < 0.05$, Figure 3C). These results suggested that, because of the presence of conformational non-RBD epitopes, full-length S protein as a booster can significantly enhance the IgG and IgG subtype response in mice, in comparison to the use of RBD protein as a booster.

Of note, the live virus neutralization assay showed that the cross-neutralizing

responses was significantly enhanced when conformational non-RBD epitopes were boosted *via* injecting the full-length S protein, in comparison to boosting RBD epitopes alone. 7.69-fold higher neutralizing antibody response against Wuhan-01 strain was elicited by full-length S protein boost, compared to RBD alone boost ($P < 0.001$, Figure 3D). Similarly, 8.24-fold and 4.02-fold higher neutralizing antibody response against Delta strain (B.1.617.2) and Omicron strain (B.1.1.529) were obtained by boosting conformational non-RBD epitopes (S_{DNA}-S-S), compared to only boosting RBD epitopes (S_{DNA}-RBD-RBD) (Figure 3D). These results demonstrated that boosting conformational non-RBD epitopes can significantly improve SARS-CoV-2 cross-neutralization.

Analyzing the distribution of neutralizing epitopes in conformational non-RBD and RBD regions.

Clarifying the spatial distribution of primary antigenic epitopes on the S protein holds critical significance in unveiling the mechanisms underpinning cross-neutralization against SARS-CoV-2 variants, particularly those mediated by the conformational non-RBD region. We conducted a comprehensive analysis of 2,397 neutralizing antibody (nAb) sequences and structures from the coronavirus antibody database (CoV-AbDab) (Raybould et al., 2021) to investigate the distributuion pattern of non-RBD and RBD neutralizing epitopes of SARS-CoV-2 (Figure 4A). After the filtration based on the standard of the immune model, antibody function, structural accessibility and variant analysis, we picked out 78 entries with crystal structures of spike antigen-neutralizing antibody complexes (S-nAbs) in the protein data bank (PDB) (Berman et al., 2003) for the epitope analysis.

We developed a new software tool called IBEIP (intelligent batch epitope identification and partitioning) for the intelligent analysis to partition S antigen regions and screen epitope sites (Methods, Identifying and partitioning epitopes of neutralizing antibody). In contrast to the traditional epitope-partition method that relied on manual processing to partition epitope regions (Yuan et al., 2021), our IBEIP can utilize an innovative iterative algorithm to intelligently partition hundreds of epitope sites at a

minus-scale processing speed. In the current study, we defined the epitope site as the antigenic residues that are contacted and buried by neutralizing antibodies (nAbs) *via* the interaction of at least one hydrogen bond in the S-nAbs. To precisely screen out epitope sites, we calculated antigenic residues that are contacted (a distance < 5 Å) or buried (a buried surface area > 0 $Å^2$) by S-nAbs from PDB(Yuan et al., 2021). In addition, hydrogen bonds (a distance between the hydrogen atom donor and acceptor < 3.2 Å) were also incorporated into the identification process of epitope sites by IBEIP.

A total of 78 S-nAbs were analyzed. Through IBEIP, we partitioned six non-RBD epitope regions (non-RBD1 to non-RBD6) and six RBD epitope regions (RBD1to RBD6) (Figures 4B, 4C, S2 and S3). It is noteworthy that five of the six non-RBD regions (non-RBD1 to non-RBD5) were located in the NTD of S protein and one spanned from NTD (residues 217-220, 278, 286-290, 294) to S1/S2 (residues 602-607) domain of the S protein (Figure 4B). Furthermore, in the six non-RBD regions we identified a total of 24 epitope sites (non-RBD1: 1 site, non-RBD2: 2 sites, non-RBD3: 2 sites, non-RBD4: 17 sites, non-RBD5: 1 sites, non-RBD6: 1 sites) (Table 1)，54 epitope sites were identified in the six RBD regions (RBD1: 27 sites, RBD2: 6 sites, RBD3: 12 sites, RBD4: 7 sites, RBD5: 1 site, RBD6: 1 site) (Table 1).

We next analysized the nAb binding frequency of the epitope regions. The binding frequency is defined as the percentage of nAbs that bind to the specific epitope region. We found that the nAb binding frequency of non-RBD4 and RBD1 were significantly higher than those of other regions, 21.79% and 34.62%, respectively (Figure 4C and Table 1). In addition, the nAb binding frequency also showed significant differences among epitope residues within the same epitope region (Figure 4C). The top 10 frequency residues of non-RBD4 were residues 144YYHKN148 (14.1%-15.38%) and 250TPGDS254 (10.26%-17.95%). The top 7 frequency residues of RBD1 were residues 481NGVEG485 (10.25%-23.08%), 490F (11.54%) and 492L (16.67%). The more important, we observed a significant overlap between the non-RBD4 region identified herein and a previously reported NTD supersite epitope region (McCallum et al., 2021; Wang et al., 2022). This overlap underscores the reliability of our antigenic epitope identification and partitioning methodology. These results indicated that non-

RBD4 and RBD1 regions might be important for conformational non-RBD and RBD domain to induce the neutralizing antibody response against SARS-CoV-2.

Quantifying the percentage of conformational epitope-specific binding antibodies and validating its contribution to neutralization.

To further validate the accuracy of our epitope identification results, we employed negative stain electron microscopy-based polyclonal epitope mapping (ns-EMPEM) to elucidate the epitopes of serum antibodies that bind to the conformational non-RBD and RBD region of SARS-CoV-2 spike protein (Bangaru et al., 2022; Bianchi et al., 2018). Polyclonal Fabs were obtained by papain digested IgGs pooled from S_{DNA}-RBD-RBD/S_{DNA}-S-S group sera (Bianchi et al., 2018). Subsequently, the resulting Fabs were complexed with the spike protein and purified using size exclusion chromatography for single-particle EM data collection. Standard EM processing was performed, including particle extraction, 2D classification, and 3D reconstruction (Bangaru et al., 2022), while extensive 3D classification was conducted to sort each Fab specificity. The spike model (PDB: 6XR8) and Fab model (PDB: 6WS6) were subsequently fitted into reconstructed 3D maps to identify epitopes of each antibody on the surface of the SARS-CoV-2 spike protein (Figure 5A). The conformation of antigen S protein manifested a prototypical homotrimer structrure (Figure S4). The 3D reconstruction of polyclonal Fabs in complex with the wild-type spike protein of SARS-CoV-2 from the S_{DNA}-RBD-RBD group (Figure 5B, left and up) and the S_{DNA}-S-S group (Figure 5B, left and down) revealed significant differences in their binding specificities. The binding responses of polyclonal Fabs to RBD were observed in the S_{DNA}-RBD-RBD group, whereas the S_{DNA}-S-S group antibodies exhibited binding to both conformational non-RBD and RBD epitopes. Moreover, our findings indicate that non-RBD-targeting antibodies approach spike protein from two distinct angles, which were labeled as 'nsEM-nonRBD1' and 'nsEM-nonRBD2' (Figure S5). In the S_{DNA}-RBD-RBD group, RBD antibodies accounted for approximately 15% of the total ~13k particles (Figure 5B, right and up). In contrast, in the S_{DNA}-S-S group, non-RBD antibodies accounted for approximately 54% of the total ~10k particles, while RBD antibodies

occupied only 9% of the total particles (Figure 5B, right and down). It can be seen that among all the antibodies induced by the S protein, there are significantly more antibodies targeting the non-RBD region than those targeting the RBD region. Building upon the above epitope region analysis (Figures 4B and 4C), most non-RBD epitope regions are located on the NTD region. We believe the significant advantage of cross-neutralization potency in the S_{DNA}-S-S group over the S_{DNA}-RBD-RBD group (Figure 3D) is attributable to the low mutational variability and the relative epitope conservation on the NTD region. Consequently, antibodies induced by these epitopes can also bind to corresponding epitopes from different mutant strains. Moreover, the higher quantity of antibodies targeting the NTD further improve its broad neutralization activity. Additionally, a list of potential contact residues between the spike protein and non-RBD antibodies were generated with an interaction distance of ⩽5Å (Figure 5C, right) (Dingens et al., 2021). However, reconstructing the RBD antibodies was more challenging, and it was not possible to identify concrete interaction residues due to the flexible nature of the RBD (Bangaru et al., 2022). Nevertheless, the analysis of EM data (2D and 3D) revealed the presence of both non-RBD and RBD antibodies.

In this study, the epitope profile identified by ns-EMPEM analysis was observed in accordance with the identified epitopes of the SARS-CoV-2 S protein (Figure 5D). By in-depth analyses of the distribution of the non-RBD epitope sites identified by ns-EMPEM within the 6 identified non-RBD epitope regions (non-RBD1 to non-RBD6), we observed that the residues of nsEM-nonRBD overlapped 45.1% with the non-RBD4 epitope region (Figure 5E). Overall, the non-RBD epitopes identified by ns-EMPEM were consistent with our identified non-RBD4 epitope region.

A pseudotyped virus neutralization assay was conducted to validate the impact of NTD-specific antibodies on the neutralizing efficacy of the serum (Figure 5F). The pseudotyped virus neutralization assay illustrated a significant reduction in the neutralizing capacity of serum samples when blocking the binding activity of NTD-specific antibodies. Specifically, the neutralization potency of serum from the S_{DNA}-S-S group decreased upon blocking with a low concentration of NTD protein (0.04 μg/μl) (Figure 5H). Furthermore, an elevation in blocking concentration of NTD protein (0.08

μg/μl) led to a significant decrease in serum neutralization potency ($P < 0.005$, Figures 5G and S6). These findings provide evidence that NTD-specific antibodies play a crucial role in enhancing the neutralization efficacy against SARS-CoV-2.

DISCUSSION

The maintenance of antigen spatial conformation is closely related to the quality of vaccine-induced antibody responses. Currently, for the construction of SARS-CoV-2 vaccines, the preservation of the spatial conformation of either full-length S or RBD antigens has been realized (Mao et al., 2022; Xu et al., 2022; Yang et al., 2023b). In constrast, conformational non-RBD antigens have still not been successfully developed yet, although several studies have highlighted the importance of conformational non-RBD antigens in fighting against SARS-CoV-2 infection (Dussupt et al., 2021; Voss et al., 2021).

One of challenges in developing conformational non-RBD antigens is that *in vitro* expression of non-RBD will significantly alter its spatial conformation (Olmedillas et al., 2023). This challenge requires us not to directly inject protein antigen to boost conformational non-RBD-specific antibodies. To solve this problem, we selected S DNA prime-S protein boost strategy. According to our analysis (details shown in Figures 5B and 5C), both S antigen-expressed plasmid and S protein can induce conformational non-RBD-specific antibody response. Moreover, DNA prime-protein boost strategy has been proven to be a robust immunization approach in our and other groups' vaccine models such as SARS-CoV-2, HIV and HBV (Burm et al., 2023; Chiang et al., 2022; Li et al., 2021). Together, DNA prime-protein boost can provide a reasonable strategy in inducing potent conformational non-RBD-specific antibody responses.

One important finding in this study is that most binding antibodies in non-RBD boost mice are located in the NTD supersite which is a conformational epitope in the non-RBD4 region, through comparing the antibody response profiles of S_{DNA}-RBD-RBD and S_{DNA}-S-S. Moreover, these non-RBD boost mice displayed a higher neutralization potency (from 3.5 to 8.24 fold) against diverse SARS-CoV-2 strains, in

comparison to the mice without non-RBD boost. Furthermore, *via* blocking the NTD-specific binding antibodies, the neutralization potency of serum samples from non-RBD boost mice significantly decreased. Such decrease of neutralization potency has a close relationship with blocking NTD-specific binding antibodies. Therefore, these results indicated that neutralizing antibodies targeting the NTD supersite play a crucial role in mediating SARS-CoV-2 cross-neutralization.

Another novelty of our study is the combination of intelligent epitope identification with electron microscopy-based (ns-EMPEM) epitope validation. To identify potentially crucial epitopes which are responsible for enhancing the cross-neutralizing capability of S-boosted animals, we developed a new intelligent iteration method (IBEIP) to analyze the electron microscope structures of SARS-CoV-2 virus bound to nAbs from the CoV-AbDab database and identify their corresponding epitope sites. By analyzing the antibody binding frequency against these epitope sites, we identified two significant epitope regions, namely non-RBD4 and RBD1. The ns-EMPEM analysis further pinpointed the pivotal epitope positions and quantified the percentage of antibodies targeting the conformational non-RBD region. The vaccinated mice with potent SARS-CoV-2 cross-neutralization obtained 54% non-RBD-specific antibody responses and 9% RBD-specific antibody responses. Notably, the ns-EMPEM analysis also indicated that non-RBD-specific Abs predominantly focused their response on the non-RBD4 region which further affirming the accuracy of our developed IBEIP approach.

In summary, this work represents a proof-of-concept investigation for the pivotal role of conformational non-RBD epitopes in enhancing cross-neutralization of SARS-CoV-2 vaccines. Our findings offer a fresh research perspective and a design strategy for next generation SARS-CoV-2 vaccines. Our approach of combining intelligent epitope identification with electron microscopy-based epitope validation enabled a rapid and accurate determination of critical epitope information for the enhanced cross-neutralzing response of conformational non-RBD region. Such an approach would also be benefit to the prevention and treatment research of other pathogens that have abundant crystal structures of antigen-antibody complexes, such as HIV or influenza.

METHOD DETAILS

Vaccine design

The Spike protein of SARS-CoV-2, spanning positions 21,563–25,384 in the viral genome, was codon-optimized for expression in 293 cell lines. Similarly, the RBD protein,encompassing positions 222,517–23,185 in the SARS-CoV-2 isolate Wuhan-Hu-1 (GenBank accession number: MN908947), underwent codonoptimization for expression in CHO-S cell lines. Codon-optimized sequences encoding the full-length spke (S) or RBD protein of SARS-CoV-2 were inserted into PVAX-1 expression plasmids, serving as DNA vaccines.

Protein expression and purification

A plasmid encoding the SARS-CoV2 S-2 S protein and RBD protein, incorporation an FC-tag for purification, was codon-optimized and synthesized by GenScript. Subsequently, these constructs were cloned into pCDNA2004. The chosen expression platforms were 293F and CHO-S cells. Transient transfection of cells was performed utilizing Hieff TransTM Liposomal Transfection Reagent (Yeasen Biotechnology) in accordance with the manufacturer's instructions. Cultures were maintained for 6 days at 37 °C and 5% CO_2. Following transfection, the culture supernatant was collected and centrifuged for 5 min at 300 × g to eliminate cells and cellular debris. The resulting supernatant underwent sterile filtrationi using a 0.22 μm vacuum filter and was subsequently stored at 4 °C until needed. Purification of the FC-tagged SARS-CoV-2 Spike protein and RBD protein was carried out employing a purification protocol employing 5 ml Protein At Beads 4FF (Smart-Lifesciences). FC tags on the S and RBD proteins were removed through treatment with Factor Xa Proteinase (Promega).

Immunizations

Female BALB/c mice, aged six to eight weeks, were sourced from the Institute of Medical Biology, Chinese Academy of Medical Sciences (CAMS), and were maintained in specific pathogen-free (SPF) conditions at the Central Animal Care Services of Institute of Medical Biology, CAMS. All mouse experiments were ethically

approved by the animal ethics committee of Institute of Medical Biology, CAMS, with the assigned review number DWSP202008021. Experimental and control animals were co-housed, and the research staff received training in animal care and handling. Approval for animal experiments was obtainedfrom the Yunnan Provincial Experimental Animal Management Association.

The mice were randomly divided into five groups (n = 5) as following: (1) 35 μg aluminum adjuvant and 10 μg Spike protein for two dose (Alu+S protein group); (2) 35 μg aluminum adjuvant and 10 μg RBD for two dose (Alu+RBD group); (3) 15 μg DNA vaccine for one dose, 35 μg aluminum adjuvant and 10 μg Spike protein for two dose (DNA prime-Alu+S protein boost group); (4) 15 μg DNA vaccine for one dose, 35 μg aluminum adjuvant, and 10 μg RBD for two dose (DNA prime-Alu+RBD protein boost group); (5) 0.9 % saline (Control group).

On day 0, mice received DNA vaccine or PBS (no prime group) or saline (Control group) through intramuscular injection. Protein vaccines or saline (Control group) were administered *via* intramuscular injection on day 14 and day 28. Ten days after the final immunization, mice were euthanized ed to collect spleens and serum samples.

Antigen-specific binding antibody assay

The analysis of Spike and RBD antibody responses was conducted using enzyme-linked immunosorbent assay (ELISA). Spike/RBD-specific IgG, IgG1, IgG2a, IgG2b, IgG3 in mice serum were quantified by ELISA. Specifically, 96-well plates were coated with Spike or RBD antigen (0.25 μg per well) and left overnight at 4 °C. Subsequently, these plates were blocked with 2% BSA for 2 h at 37 °C. After blocking, the plates were washed three times with PBST (Phosphate buffer saline (PBS) with 5‰ Tween 20), and100 μl mice serum was added per well. Incubation was carried out at 37 °C for 1 h. Following incubation, the plates were washed three times with PBST. Each well of 96-well plate was then treated with 100 μl HRP-labeled goat anti-mouse IgG, IgG1, IgG2a, IgG2b, IgG3, IgM binding antibody at 37 °C for 1 h. Following another three washes with PBST, 50 μl 3,3′,5,5′-tetramethylbenzidine (TMB; Sigma) was added to each well. The reaction was stopped with 50 μl 0.05% H_2SO_4, and the absorbance value at 450 nm

and 630 nm wavelengths were determined using an ELISA plate reader (Tecan, San Jose, CA).

Live virus neutralization assay.

Neutralizing antibody detection was conducted using a live virus infection platform. Three SARS-CoV-2 live virus types (Wuhan-Hu-1, B.1.1.7 and B.1.617.2) were obtained from the Institute of Medical Biology, Chinese Academy of Medical Sciences (CAMS). Serum serial dilutions were incubated with 2000 PFU of an early SARS-CoV-2 isolate in 100 µl OptiPro medium supplemented with 1x GlutaMAX (both Gibco) for 1 h at 37 °C. The mixture was then added onto a confluent monolayer of Vero E6 cells (seeded the day before at 10^4 cells per well in a 96-well plate). After 1 h, the mixture was removed, and 100 µl OptiPro medium supplemented with 1x GlutaMAX (both Gibco) was added. After 24 h of incubation at 37 °C and 5% CO_2, cells were fixed with 100 µl 4% paraformaldehyde for 20 min at room temperature (RT) and permeabilized with 100 µl 0.5% Triton X-100 in PBS for 15 min at RT. Following a blocking step with 100 µl 5% skimmed milk in PBS for 1 h at RT, cells were stained with purified immunoglobulins from a SARS-CoV-2 convalescent patient in 2% skimmed milk for 1 h at 4 °C. After three washing steps with 200 µl PBS, 100 µl of anti-human IgG FITC (1:200, Jackson Immunoresearch) diluted in 2% skimmed milk were added and incubated for 1 h at 4 °C in the dark. After another three washing steps with 200 µl PBS, plaques were counted using an ELISPOT reader and analysed with CTL Immunospot software (Cellular Technology limited BioSpot). Infected wells without serum were used as a reference to determine the 75% plaque reduction neutralization titre (PRNT75).

Pseudotyped virus neutralization assay.

SARS-CoV-2 pseudotyped virus (Wuhan-Hu-1) was obtained from the Institute of Medical Biology, Chinese Academy of Medical Sciences (CAMS). Transfer 100 µl DMEM (+ 10% FBS) to 96-well round bottom plate. Transfer 47 µl DMEM (+ 10% FBS) and 3 µl serum to column 1. Transfer 50 µl serum from column 1 into column 2

and mix thoroughly. Similarly transfer 50 µl from column 2 to column 3, column 3 to column 4, column 4 to column 5, column 5 to column 6. After mixing in column 6, discard 50 µl of serum dilution. Transfer 50 µl of pseudotyped viruses into the serum dilution in the round bottom 96-well plate (except for the No virus control wells)and mix well. Place the plate into a 37 °C and 5% CO_2 incubator for 1 hour. Resuspend and count 293T-hACE2 cells in DMEM (+ 10% FBS). Dilute the cell suspension to 2 x 10^5 cells/ml and transfer 100 µl into each well of 96-well flat bottom plate using a multichannel pipette. Put the 96-well plate into an incubator set at 37 °C and 5% CO_2 incubator for 48 h. Remove the medium from the wells. Add 20 µl/well of 1x luciferase cell culture lysis reagent (Promega). Add 100 µl of Luciferase Assay reagent (Promega) to each well. Meaure the light produced (BioTek: CYTATION).

Serum IgG isolation and digestion

For IgG isolation from the serum , the following procedure was employed. Heat 500 µl of mouse serumat 56 ℃and then incubated the heated serum with 1 ml of washed Protein-G resin (GenScript L00209) overnight at 4°C. Washing the resin complex three times with PBS through centrifugation. Elute the complex with 5 ml of 0.1 M glycine buffer at pH 2.0. Immediately neutralize the eluate with 4 ml of 1 M Tris-HCl (pH 8.0) and filtered the neutralized eluate using a 0.2 µm pore filter. Buffer exchanged the elution to PBS using 30-kDa cut-off Amicon ultrafiltration units.For Fab preparation: incubate 500 µg of concentrated polyclonal IgG samples with papain (Sigma Aldrich P3125) in digestion buffer (100 mM Tris, 2 mM EDTA, 10 mM L-Cysteine, pH 7.4) for approximately 4 h in a 37°C incubator. Add iodoacetamide (Sigma Aldrich I1149-25G) to quench the digest. Then concentrate the digestion and buffer-exchanged to TBS using 10-kDa cut-off Amicon ultrafiltration units. Assess the digestion for purity using SDS-polyacrylamide gel electrophoresis.

Identifying and partitioning epitopes of neutralizing antibody

We gathered information on antibodies targeting and neutralizing the spike protein of SARS-CoV-2 from the Coronavirus Antibody Database (CoV-AbDab:

http://opig.stats.ox.ac.uk/webapps/covabdab/) through filtering. The structures of neutralizing antibodies bound to the SARS-CoV-2 spike protein were obtained from the Protein Data Bank (PDB: https://www.rcsb.org/).

To efficiently and accurately classify hundreds of epitope residues targeted by various neutralizing antibodies, we developed a method composed of three iterative cycles. In the initial cycle, we start with the epitope residues of a randomly selected neutralizing antibody. These epitope residues are merged with the epitope residues of other antibodies if the overlapping ratio between the merged set and the epitope residues of another antibody is no less than 0.9. If there are no epitope residues meeting the merger criteria, the process concludes. We then restart again with the epitope residues of a randomly selected antibody from the remaining antibodies until all antibodies are processed. After completing the first cycle, the output becomes the input for the second iterative process, repeated three times. In this process, we reduce the overlapping ratio to 0.8. Finally, the output from the second iterative process serves as input for the last cycle, repeated only two times, with the overlapping ratio reduced to 0.6. The number of final epitope regions decreases with the reduction of the overlapping ratio, and reducing the number of iterative cycles increases the number of final epitope regions.

The epitope site of a neutralizing antibody is defined as the antigen residues contacted and buried by the neutralizing antibody. A contacted epitope residue refers to an antigen residue that contacts the antibody within a distance of 5 Å in the spike-antibody complex, while the buried epitope is defined as an antigen residue with a buried surface area (BSA) greater than 0 $Å^2$. Hydrogen bonds between the antigen and antibody were calculated using PyMOL.

In summary, our method enables the rapid and accurate classification of hundreds of epitope residues targeted by different neutralizing antibodies. The efficiency of our method stems from the iterative cycle that merges epitope residues, reducing the time and complexity of manual residue comparison. The accuracy results from the thoroughness of the iterative cycle, ensuring all epitope residues are considered.

Preparation of Fab-spike complexes for ns-EMPEM

Fab-spike complexes were generatedthrough the incubation of 15 μg of spike protein with 500 μg of polyclonal Fabs overnight at 4 ℃. Subsequently, the complexes were subjected to purification using a Superdex 200 Increase 10/300 columnwith UV absorbance at 215 nm on Akta Pure system (cytiva). The purification was performed in tris-buffered saline (TBS) buffer. Fractions containing the spike-Fab complexes were collected and concentrated using 10-kDa cutoff Amicon ultrafiltration units. and the concentrated complexes were than immediately utilized for preparing ns-EMPEM grids.

Ns-EMPEM sample preparation and data collection

In the ns-EMPEM analysis, antibodies were examined using spike-Fab complexes. The final concentration of the collected fraction was approximatedly 0.015 μg/μL. Complexes were diluted to 0.015 μg/ml in 1× Tris-buffered saline and 3.5μl applied to a 200 mesh Cu grid (Zhongjingkeyi (Beijing) Films Technology Co.,Ltd) blotted with filter paper, and stained with 0.7% uranyl formate (Electron Microscopy Sciences. 22400. USA). Micrographs were collected ~100-120 on a JEOL JEM-2100F high-resolution transmission Electron microscope operating at 200 kV with a camera at ×30,000 magnification using the serial EM automated image collection software. EM-map reconstruction was performed using relion 3.1.3, and the maps were aligned and displayed using Chimera. Ns-EM density maps were deposited under EMD-xxxxx.

ACKNOWLEDGMENTS

We thank the Science and Technology Plan-biological medical special project of Yunnan Province (202302AA310005), the Basic Research Program of Yunnan Province (202101AS070051, 202201AU070152, 202002AA100009, 202101AU070126), Leading Medical Talents Program of Health Commission of Yunnan Province (L-2018013), the Young and Middle Aged Academic and Technical Leaders Program of Yunnan Province (202005AC160010), the National Natural Science Foundation of China (82304307), the National Basic Research Program of China (2020YFA0710700), the Fundamental Research Funds for the Central

Universities (3332022073) for financial supports.

AUTHOR CONTRIBUTIONS

Y. Liu, Y. R. Yang, and C. Chen led the project, designed the experiments, interpreted the data and drafted the manuscript. Y. F. Ma implemented the python code, analyzed and interpreted data from PDB and CoV-AbDab, and drafted the manuscript. Y. F. Ma, B. Xie, K. Chen, J. Zhu and X. He carried out the experiments and data analysis. All authors discussed the results and commented on the manuscript.

DECLARATION OF INTERESTS

The authors declare no competing interests.

Figures. 1-5.

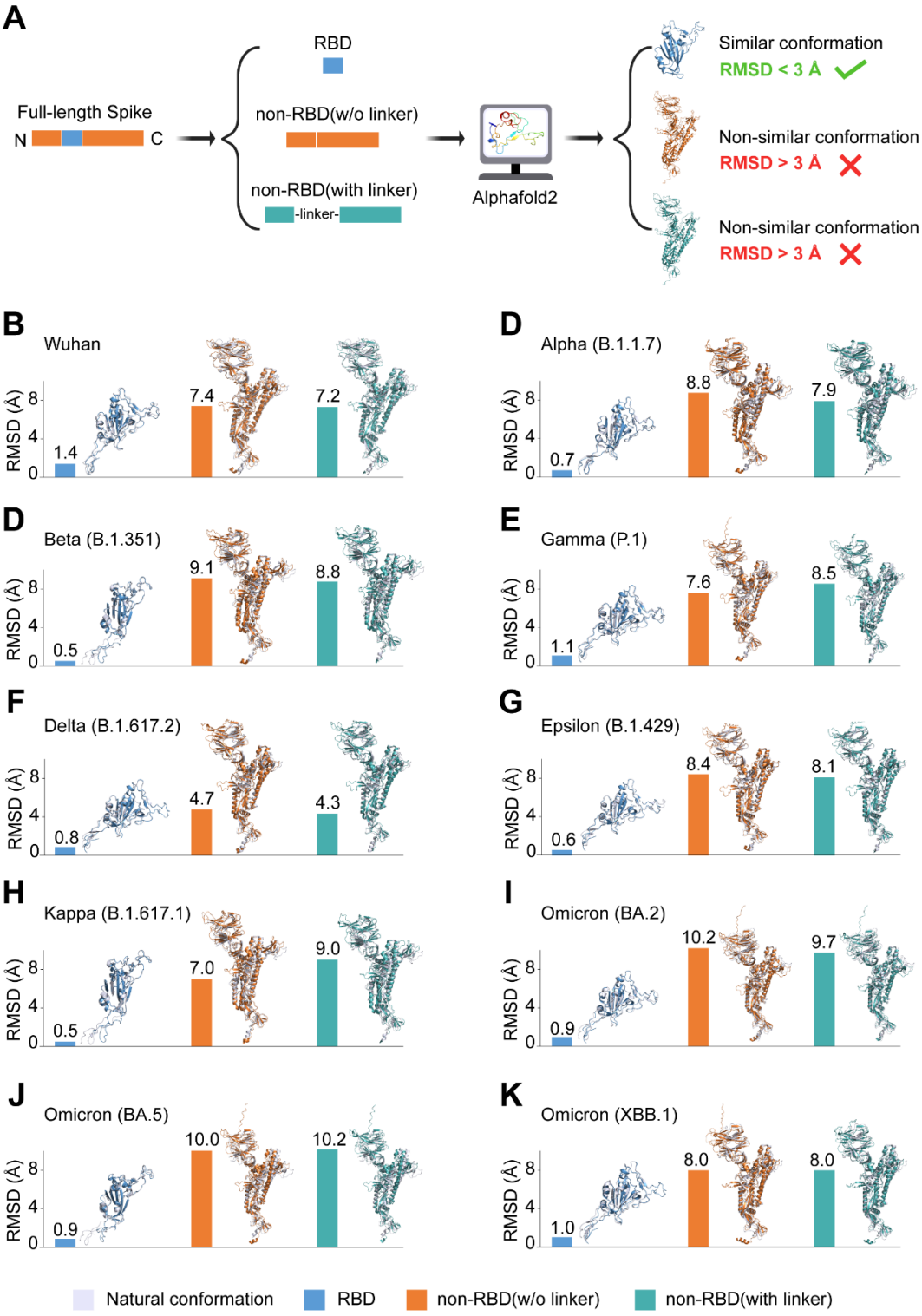

Figure 1. Structure analysis of conformational non-RBD and RBD subunits

(A) Selecton strategy of conformational non-RBD and RBD protein vaccines.

(B-K) Structural comparision of predicted non-RBD and RBD epitope vaccines with natural conformation of full-length S antigen.

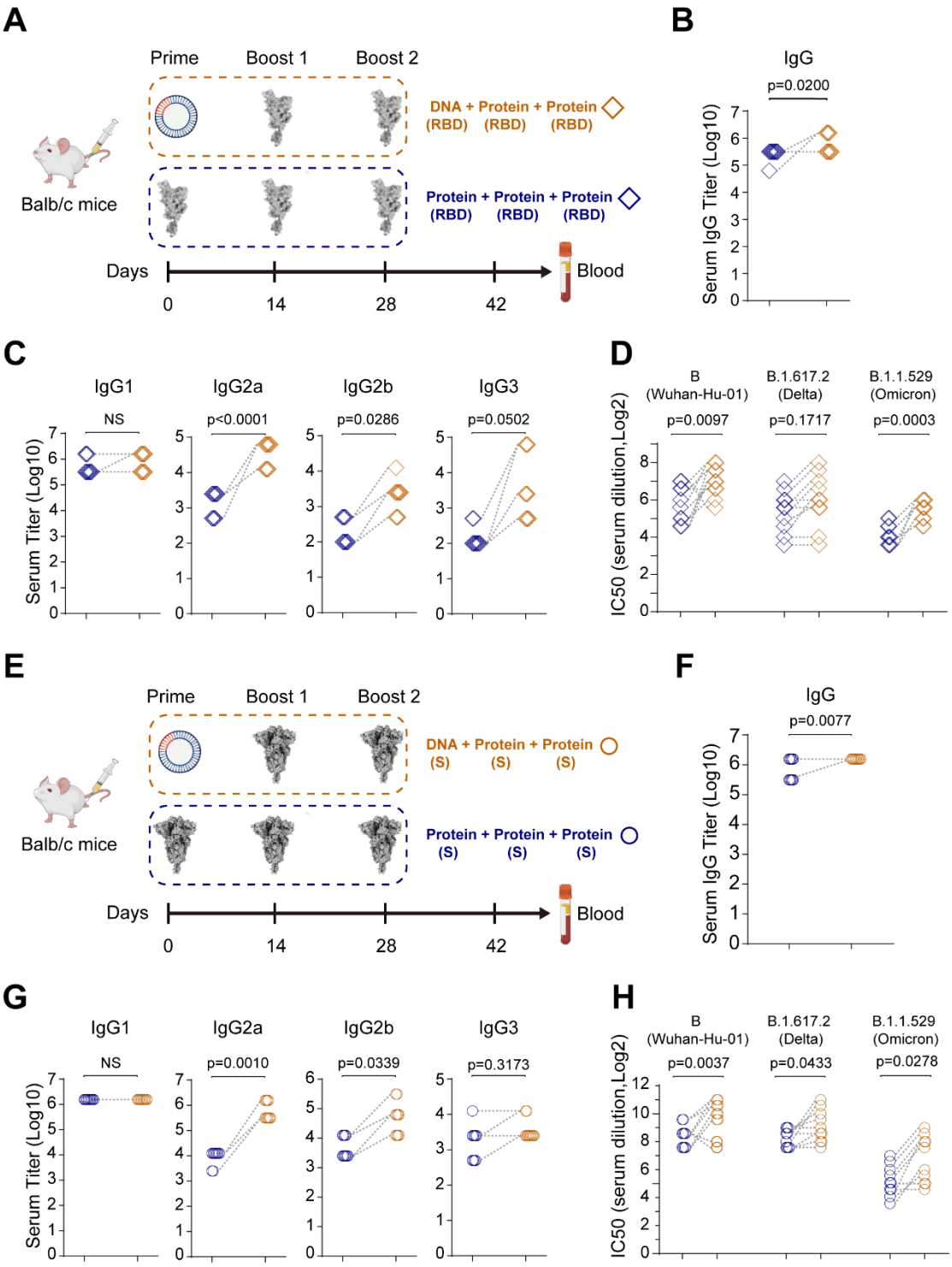

Figure 2. Humoral responses after intramuscular immunization with DNA vaccines and Protein vaccines

(A) BALB/c mice were immunized by intramuscular injection with SARS-CoV-2 RBD protein (the immunization given in two shots two weeks apart). Mice from the prime-boost groups were primed two weeks before by intramuscular injection S-encoding DNA plasmids (15 μg per plasmid). Serum antibody responses were analysed fourteen

days after the immunization.

(B) RBD-specific IgG was assessed by ELISA.

(C) RBD-specific IgG subtypes were assessed by ELISA.

(D) Live virus neutralization titres were determined by *in vitro* neutralization assays.

(E) BALB/c mice were immunized by intramuscular injection with SARS-CoV-2 full-length S protein (the immunization given in two shots two weeks apart). Mice from the prime-boost groups were primed two weeks before by intramuscular injection of S-encoding DNA plasmids (15 μg per plasmid). Serum antibody responses were analysed fourteen days after the immunization.

(F) S-specific IgG was assessed by ELISA.

(G) S-specific IgG subtypes were assessed by ELISA.

(H) Live virus neutralization titres were determined by *in vitro* neutralization assays. Each rhombus (b-d) or circle (f-h) represents one sample, n = 10. Data were analysed by T-test.

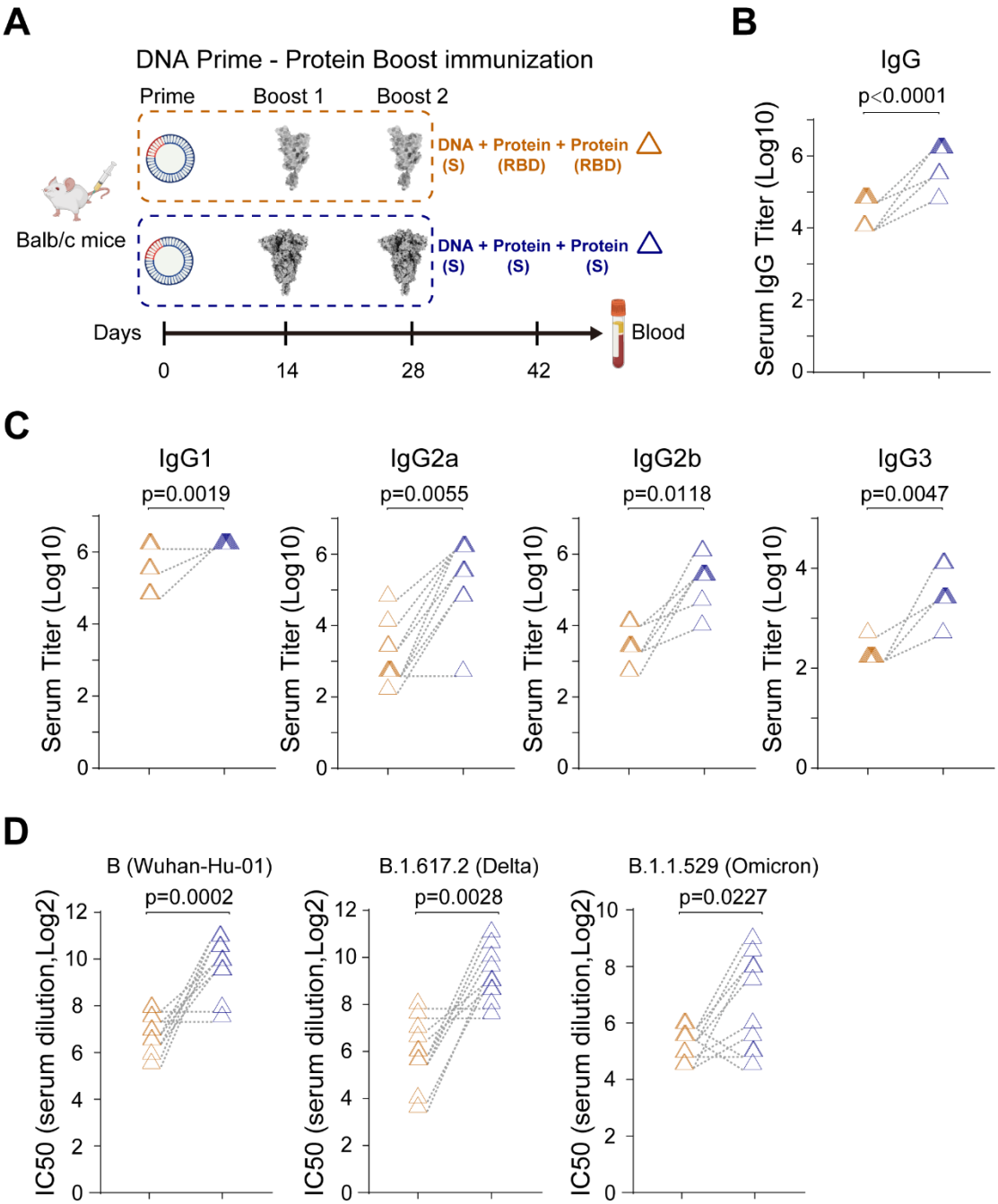

Figure 3. Humoral responses after intramuscular immunization with DNA Prime and two different Protein vaccines

(A) BALB/c mice were primed by intramuscular injection of S-encoding DNA plasmids (15 μg per plasmid). Then mice were immunized by intramuscular injection two weeks later with RBD protein or Spike protein (the immunization given in two shots two weeks apart). The mice were primed two weeks before by intramuscular injection of S-encoding DNA plasmids (10 μg per plasmid). Serum antibody responses were analysed fourteen days after the immunization.

(B) Spike-specific IgG was assessed by ELISA.

(C) Spike-specific IgG subtypes were assessed by ELISA.

(D) Live virus neutralization titres were determined by *in vitro* neutralization assays.

Each triangle (b-d) represents one sample, n = 10. Data were analysed by T-test.

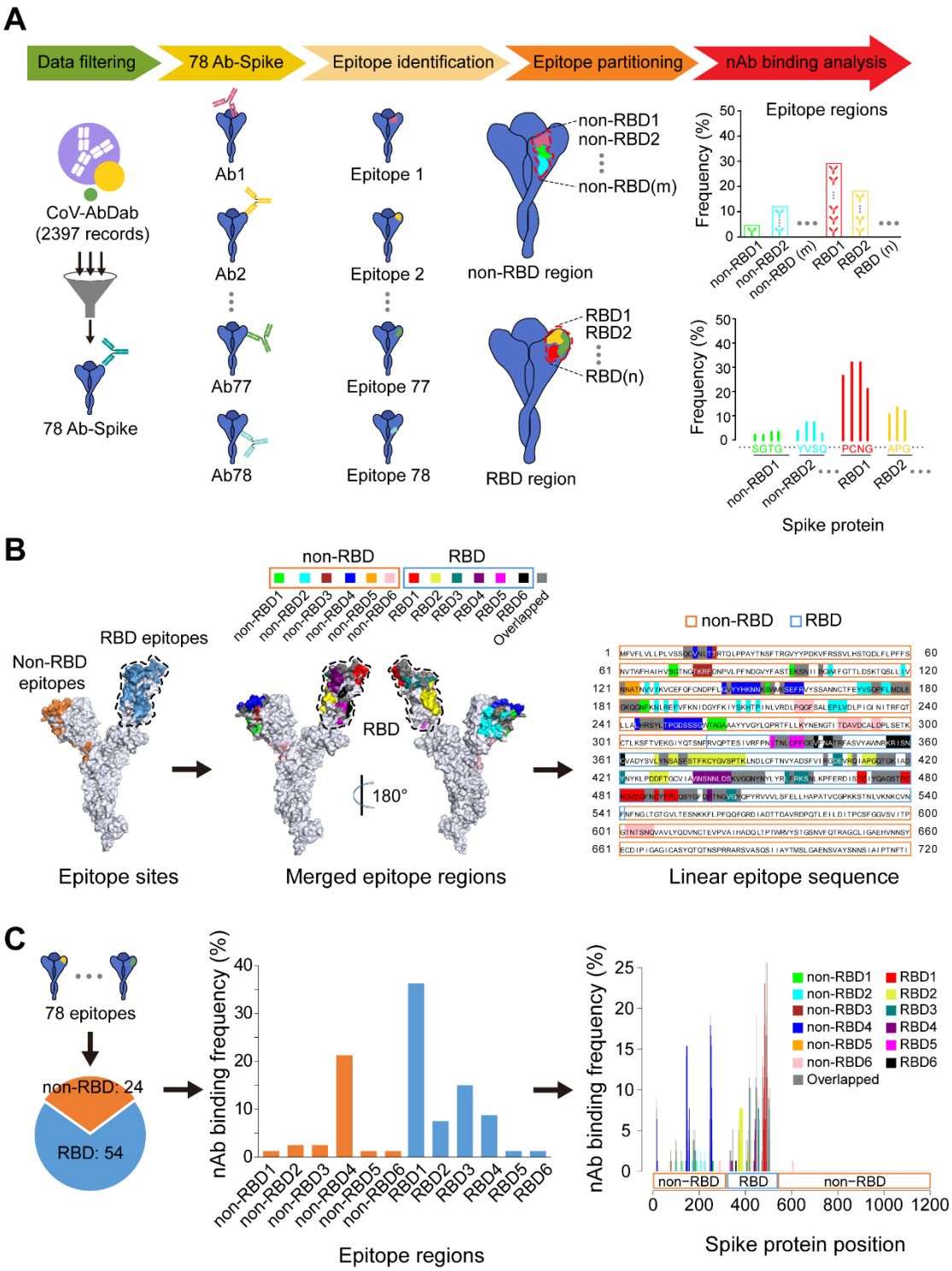

Figure 4. Non-RBD and RBD epitopes being identified within the spike protein of SARS-CoV-2

(A) Non-RBD and RBD epitope identification flow chart.

(B) Left, identified non-RBD and RBD epitopes. Middle, non-RBD and RBD epitope regions projected onto protein 3D structures. Right, linear sequence of 12 epitope regions.

(C) Left, ratio of non-RBD and RBD epitope sites. Middle, nAb binding frequency of the non-RBD and RBD epitope regions. Right, Ab binding frequency of epitope residues within the different epitope regions. The gray vertical line represents epitope residues overlapped by at least two epitope regions.

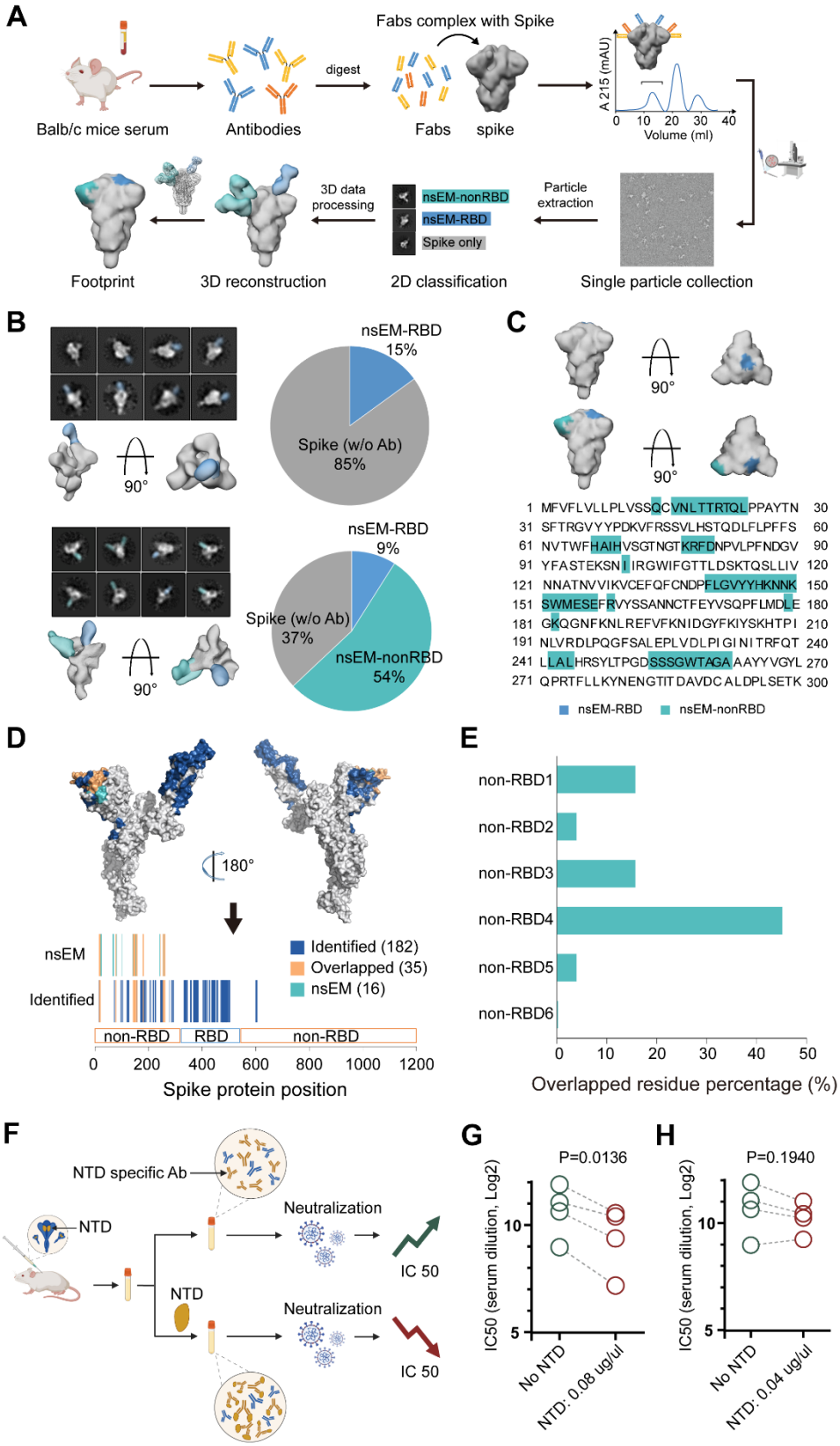

Figure 5. Ns-EMPEM analysis of polyclonal Fabs from vaccinated mouse sera complexed with SARS-CoV-2 spikes

(A) Schematic diagram of ns-EM polyclonal epitope mapping (EMPEM) analysis.

(B) Representative 2D classes, side and top views of the 3D reconstructions from ns-EMPEM analysis of SARS-CoV-2 spikes complexed with polyclonal Fabs isolated from DNA(S)-RBD-RBD and DNA(S)-S-S vaccination groups. Pie charts show the proportion of pAbs targeting the SARS-CoV-2 nsEM-nonRBD (sea green), nsEM-RBD (blue), and spike (w/o Ab) (gray).

(C) Surface representation of each antibody epitope on the SARS-CoV-2 spike. The spike trimer with three "down" RBDs is adapted from PDB ID 6XR8. The epitope residues involved in NTD binding are labeled with their respective color. Interaction residues in NTD are defined by a 5 Å distance cut-off.

(D) Comparison between identified and ns-EMPEM epitopes.

(E) The percentage of ns-EMPEM non-RBD epitopes overlapped with the identified non-RBD epitope regions.

(F) Schematic diagram of the experiment to evaluate the influence of NTD-specific Abs on neutralization against pseudotyped virus.

(G) Pseudotyped virus neutralization titres of serum with or without NTD protein incubation (0.08 μg/μl).

(H) Pseudotyped virus neutralization titres of serum with or without NTD protein incubation (0.04 μg/μl). Data were analysed by T-test.

Table 1. The epitope residues and regions within the non-RBD and RBD regions on the spike protein of SARS-CoV-2.

Antigen	Epitope regions	Ab binding frequency	Overlapped site positions	Unique site positions
RBD	RBD1	34.62%	403, 416, 417, 444-450, 456, 473-478, 486, 487, 489, 493-496, 498, 505	470, 471, 479-485, 488, 490-492
	RBD2	7.69%	369, 370, 373, 374, 409, 414-417, 420, 460	368, 371, 372, 375-386, 408, 411-413, 427-430
	RBD3	15.38%	369, 370, 403, 409, 414-417, 420, 449, 456, 460, 473-478, 486, 487, 489, 493-496, 498, 500-502, 505	405, 406, 421, 455, 457-459, 503, 504
	RBD4	8.97%	345, 346, 373, 374, 444-450, 498, 500-502	436-443, 499
	RBD5	1.28%	333-335, 339, 340	332, 336-338
	RBD6	1.28%	333-335, 339, 340, 345, 346	341, 343, 344, 356-361
Non-RBD	non-RBD1	1.28%	97-99, 150, 152, 178-184, 245-249	71, 72, 96, 151, 185, 186, 259-262
	non-RBD2	2.56%	99, 102, 121, 173, 174, 177-180, 182	104, 119, 126, 128, 170-172, 175, 176, 188, 190, 192, 205, 207, 209, 224-227
	non-RBD3	2.56%	14, 15, 17, 18, 143, 247	20, 76-79
	non-RBD4	21.79%	14, 15, 17, 18, 143, 150, 152, 154, 245-249	16, 19, 142, 144-149, 155-158, 244, 250-257
	non-RBD5	1.28%	97-99, 102, 121, 154, 173, 174, 177, 178, 180-184	122-124

non-RBD6	1.28%	/	217-220, 278, 286-290, 293, 294, 602-607

Figures. S1-6

Figure S1. Structure comparision of predicted non-RBD and RBD epitope vaccines with spatial conformation of full-length S antigen for 8 SARS-CoV-2 variants.

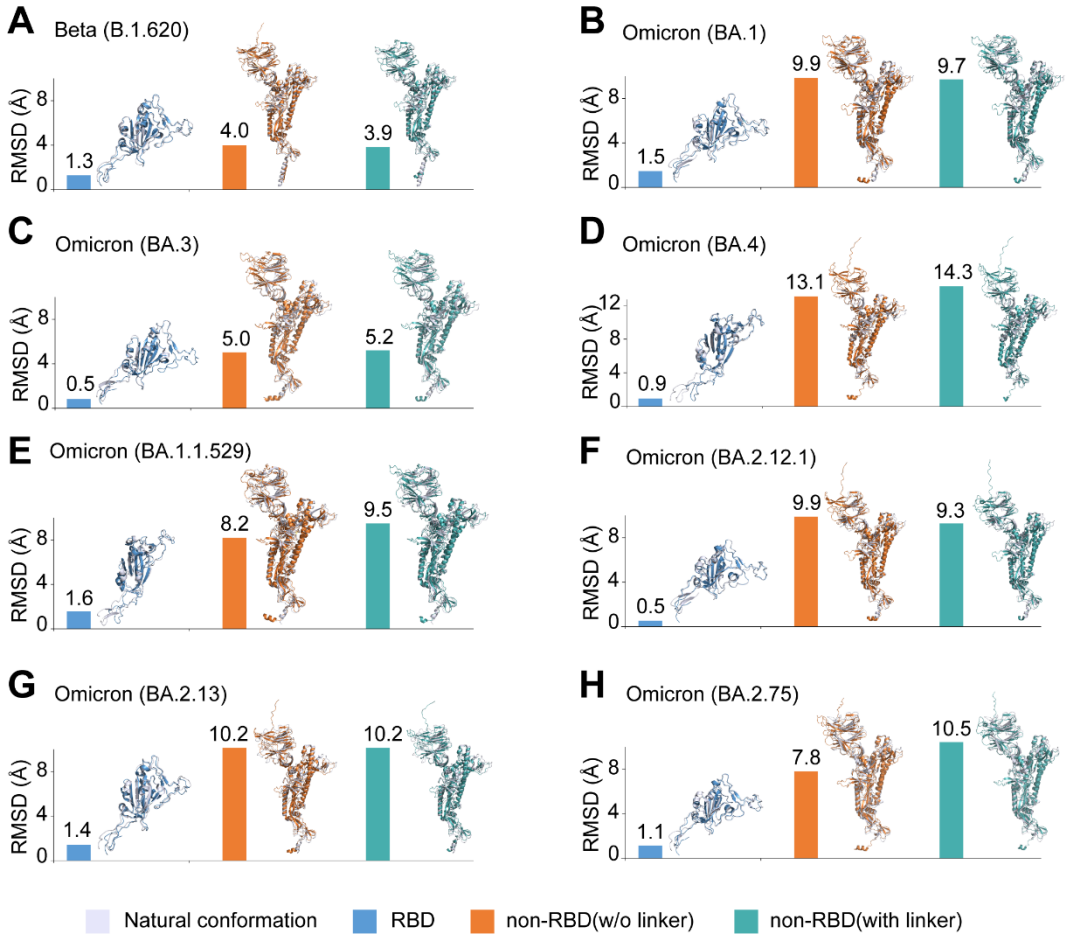

Figure S2. The six identified regions of non-RBD epitope.

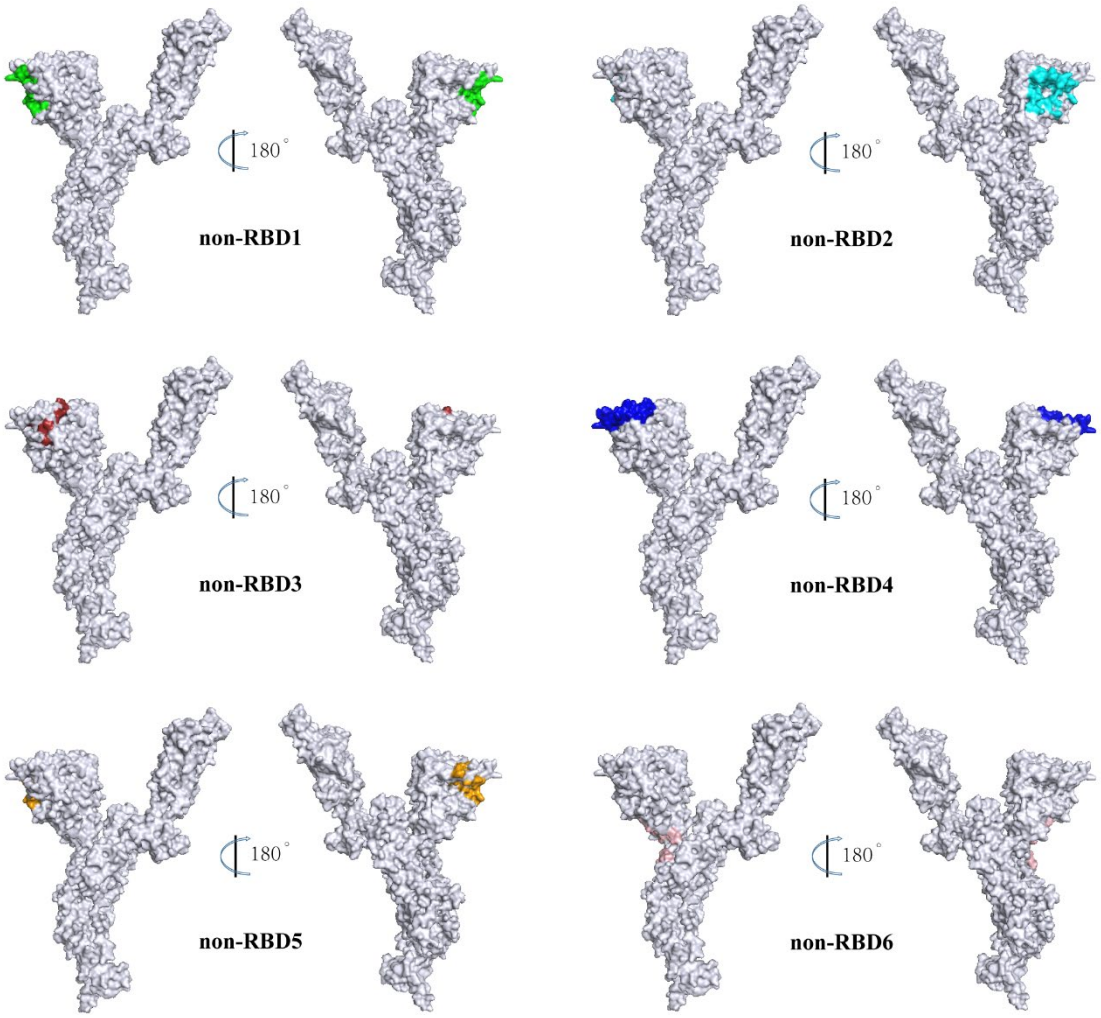

Figure S3. The six identified regions of RBD epitope.

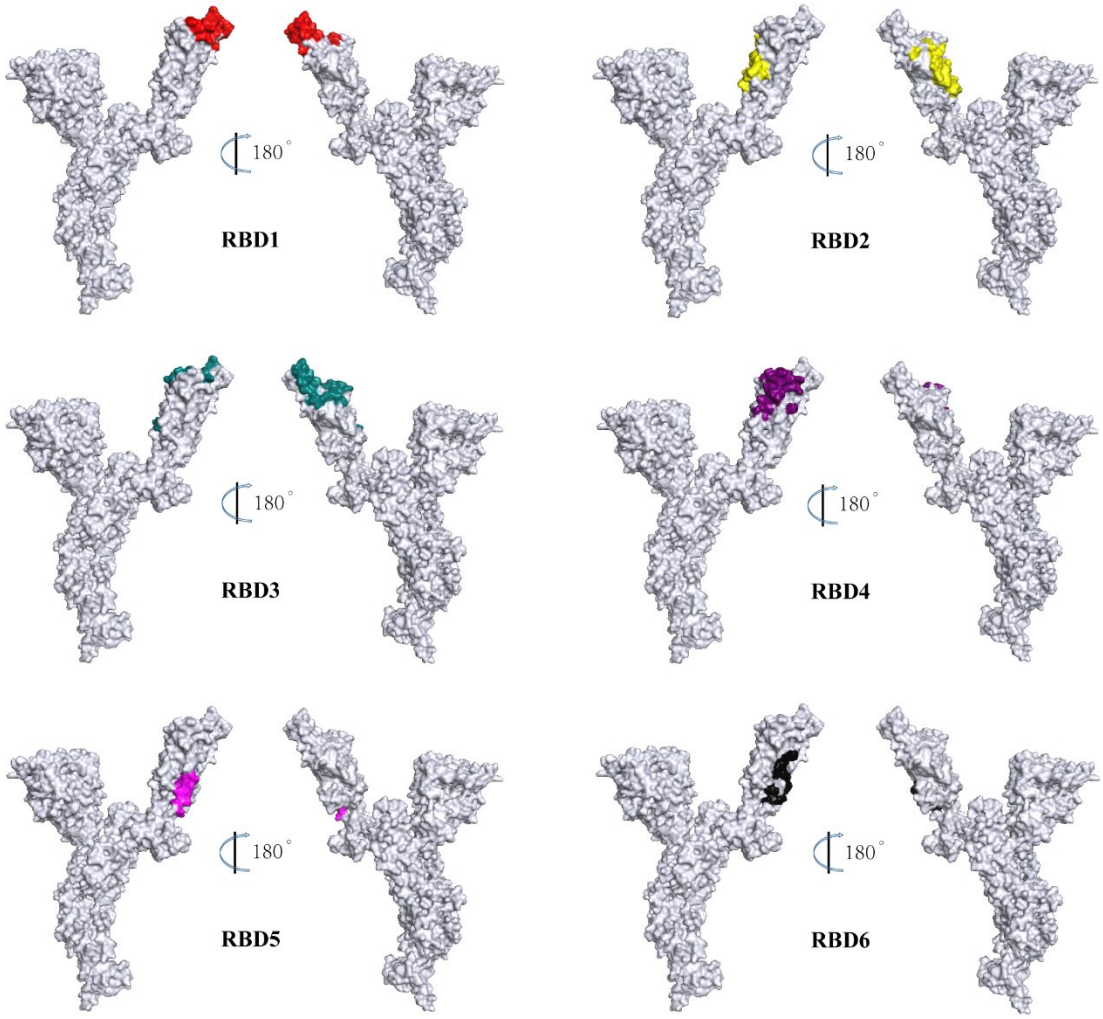

Figure S4. The 3D reconstructions from ns-EMPEM analysis of SARS-CoV-2 spike protein.

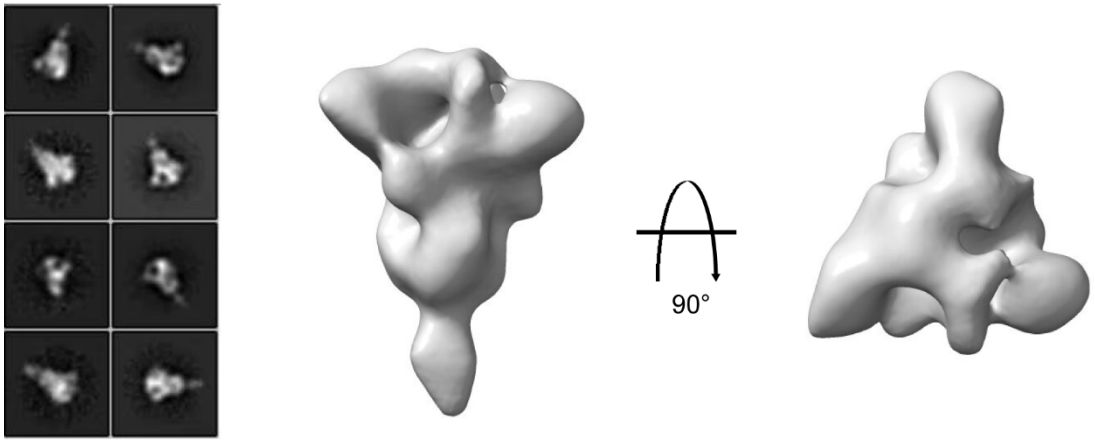

Figure S5. The ns-EMPEM analysis revealed two non-RBD epitope regions.

(A) Representative 2D classes, side and top views of the 3D reconstructions from ns-EMPEM analysis of SARS-CoV-2 spikes complexed with polyclonal Fabs isolated from DNA(S)-RBD-RBD and DNA(S)-S-S vaccination groups. Pie charts show the proportion of pAbs targeting the SARS-CoV-2 nsEM-nonRBD1 (teal), nsEM-nonRBD2 (cerulean), nsEM-RBD (blue), and spike (w/o Ab) (gray).

(B) Surface representation of each antibody epitope on the SARS-CoV-2 spike. The spike trimer with three "down" RBDs is adapted from PDB ID 6XR8. The epitope residues involved in NTD binding are labeled with their respective color. Interaction residues in NTD are defined by a 5 Å distance cut-off.

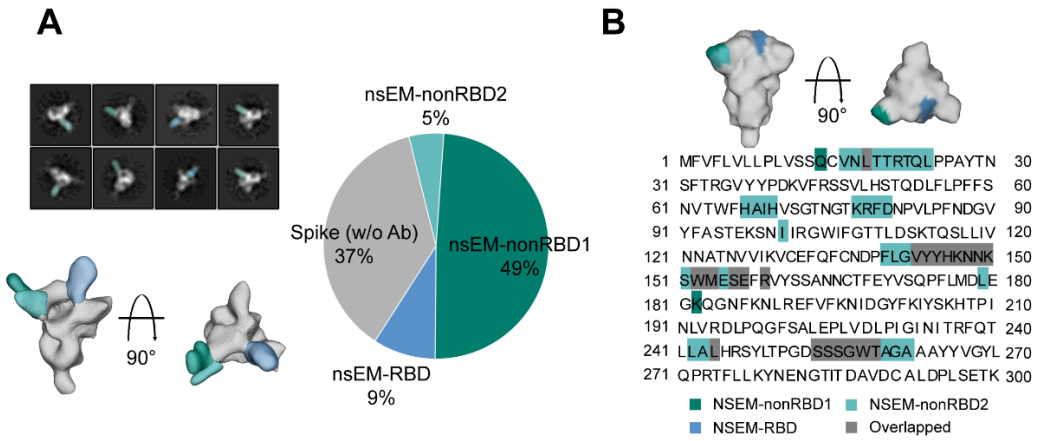

Figure S6. Pseudotyped virus neutralization titres of serum with different NTD protein concentration.

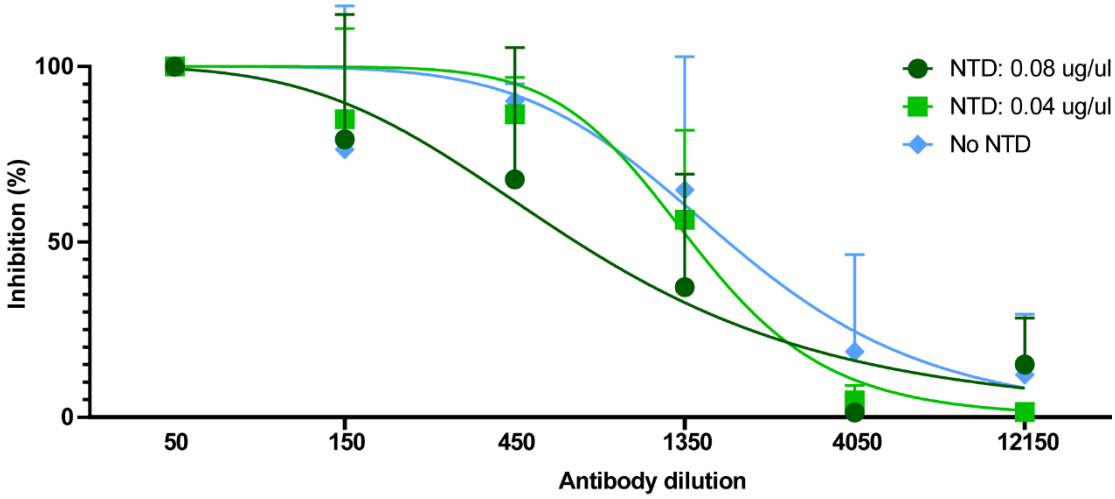

REFERENCES

Bangaru, S., Antanasijevic, A., Kose, N., Sewall, L.M., Jackson, A.M., Suryadevara, N., Zhan, X., Torres, J.L., Copps, J., de la Peña, A.T., *et al.* (2022). Structural mapping of antibody landscapes to human betacoronavirus spike proteins. Sci Adv *8*, eabn2911.

Bangaru, S., Ozorowski, G., Turner, H.L., Antanasijevic, A., Huang, D., Wang, X., Torres, J.L., Diedrich, J.K., Tian, J.H., Portnoff, A.D., *et al.* (2020). Structural analysis of full-length SARS-CoV-2 spike protein from an advanced vaccine candidate. Science *370*, 1089-1094.

Berman, H., Henrick, K., and Nakamura, H. (2003). Announcing the worldwide Protein Data Bank. Nature structural biology *10*, 980.

Bianchi, M., Turner, H.L., Nogal, B., Cottrell, C.A., Oyen, D., Pauthner, M., Bastidas, R., Nedellec, R., McCoy, L.E., Wilson, I.A., *et al.* (2018). Electron-Microscopy-Based Epitope Mapping Defines Specificities of Polyclonal Antibodies Elicited during HIV-1 BG505 Envelope Trimer Immunization. Immunity *49*, 288-300.e288.

Burm, R., Maravelia, P., Ahlen, G., Ciesek, S., Caro Perez, N., Pasetto, A., Urban, S., Van Houtte, F., Verhoye, L., Wedemeyer, H., *et al.* (2023). Novel prime-boost immune-based therapy inhibiting both hepatitis B and D virus infections. Gut *72*, 1186-1195.

Cai, Y., Zhang, J., Xiao, T., Peng, H., Sterling, S.M., Walsh, R.M., Jr., Rawson, S., Rits-Volloch, S., and Chen, B. (2020). Distinct conformational states of SARS-CoV-2 spike protein. Science *369*, 1586-1592.

Cao, F., Peng, S., An, Y., Xu, K., Zheng, T., Dai, L., Ogino, K., Ngai, T., Xia, Y., and Ma, G. (2023). Inside-out assembly of viral antigens for the enhanced vaccination. Signal transduction and targeted therapy *8*, 189.

Chen, X., Zaro, J.L., and Shen, W.C. (2013). Fusion protein linkers: property, design and functionality. Advanced drug delivery reviews *65*, 1357-1369.

Chi, X., Yan, R., Zhang, J., Zhang, G., Zhang, Y., Hao, M., Zhang, Z., Fan, P., Dong, Y., Yang, Y., *et al.* (2020). A neutralizing human antibody binds to the N-terminal domain of the Spike protein of SARS-CoV-2. Science *369*, 650-655.

Chiang, C.Y., Chen, M.Y., Hsu, C.W., Liu, C.Y., Tsai, Y.W., Liao, H.C., Yan, J.Y., Chuang, Z.S., Wang, H.I., Pan, C.H., *et al.* (2022). Induction of high affinity

monoclonal antibodies against SARS-CoV-2 variant infection using a DNA prime-protein boost strategy. Journal of biomedical science *29*, 37.

Cox, M., Peacock, T.P., Harvey, W.T., Hughes, J., Wright, D.W., Consortium, C.-G.U., Willett, B.J., Thomson, E., Gupta, R.K., Peacock, S.J.*, et al.* (2023). SARS-CoV-2 variant evasion of monoclonal antibodies based on in vitro studies. Nature reviews. Microbiology *21*, 112-124.

Dai, L., Gao, L., Tao, L., Hadinegoro, S.R., Erkin, M., Ying, Z., He, P., Girsang, R.T., Vergara, H., Akram, J.*, et al.* (2022). Efficacy and Safety of the RBD-Dimer-Based Covid-19 Vaccine ZF2001 in Adults. The New England journal of medicine *386*, 2097-2111.

Dai, L., Zheng, T., Xu, K., Han, Y., Xu, L., Huang, E., An, Y., Cheng, Y., Li, S., Liu, M.*, et al.* (2020). A Universal Design of Betacoronavirus Vaccines against COVID-19, MERS, and SARS. Cell *182*, 722-733 e711.

Dingens, A.S., Pratap, P., Malone, K., Hilton, S.K., Ketas, T., Cottrell, C.A., Overbaugh, J., Moore, J.P., Klasse, P.J., Ward, A.B., and Bloom, J.D. (2021). High-resolution mapping of the neutralizing and binding specificities of polyclonal sera post-HIV Env trimer vaccination. Elife *10*.

Dussupt, V., Sankhala, R.S., Mendez-Rivera, L., Townsley, S.M., Schmidt, F., Wieczorek, L., Lal, K.G., Donofrio, G.C., Tran, U., Jackson, N.D.*, et al.* (2021). Low-dose in vivo protection and neutralization across SARS-CoV-2 variants by monoclonal antibody combinations. Nat Immunol *22*, 1503-1514.

Gainza, P., Wehrle, S., Van Hall-Beauvais, A., Marchand, A., Scheck, A., Harteveld, Z., Buckley, S., Ni, D., Tan, S., Sverrisson, F.*, et al.* (2023). De novo design of protein interactions with learned surface fingerprints. Nature *617*, 176-184.

Gobeil, S.M., Janowska, K., McDowell, S., Mansouri, K., Parks, R., Stalls, V., Kopp, M.F., Manne, K., Li, D., Wiehe, K.*, et al.* (2021). Effect of natural mutations of SARS-CoV-2 on spike structure, conformation, and antigenicity. Science *373*.

Gu, H., Chen, Q., Yang, G., He, L., Fan, H., Deng, Y.Q., Wang, Y., Teng, Y., Zhao, Z., Cui, Y.*, et al.* (2020). Adaptation of SARS-CoV-2 in BALB/c mice for testing vaccine efficacy. Science *369*, 1603-1607.

Huang, M., Wu, L., Zheng, A., Xie, Y., He, Q., Rong, X., Han, P., Du, P., Han, P., Zhang, Z., *et al.* (2022). Atlas of currently available human neutralizing antibodies against SARS-CoV-2 and escape by Omicron sub-variants BA.1/BA.1.1/BA.2/BA.3. Immunity *55*, 1501-1514 e1503.

Huang, Y., Chen, X., Zhang, J., Tian, W., Liu, S., Chun-Yee Tam, R., Yang, C., and Song, Y. (2023). Aptamer-based strategies against SARS-CoV-2 viruses. BMEMat *1*, e12024.

Impagliazzo, A., Milder, F., Kuipers, H., Wagner, M.V., Zhu, X., Hoffman, R.M., van Meersbergen, R., Huizingh, J., Wanningen, P., Verspuij, J., *et al.* (2015). A stable trimeric influenza hemagglutinin stem as a broadly protective immunogen. Science *349*, 1301-1306.

Li, H., Wang, S., Hu, G., Zhang, L., Liu, S., and Lu, S. (2021). DNA priming immunization is more effective than recombinant protein vaccine in eliciting antigen-specific B cell responses. Emerging microbes & infections *10*, 833-841.

Liu, L., Wang, P., Nair, M.S., Yu, J., Rapp, M., Wang, Q., Luo, Y., Chan, J.F., Sahi, V., Figueroa, A., *et al.* (2020). Potent neutralizing antibodies against multiple epitopes on SARS-CoV-2 spike. Nature *584*, 450-456.

Lu, M., Chamblee, M., Zhang, Y., Ye, C., Dravid, P., Park , J.G., Mahesh, K., Trivedi, S., Murthy, S., Sharma, H., *et al.* (2022). SARS-CoV-2 prefusion spike protein stabilized by six rather than two prolines is more potent for inducing antibodies that neutralize viral variants of concern. Proceedings of the National Academy of Sciences of the United States of America *119*, e2110105119.

Mao, T., Israelow, B., Pena-Hernandez, M.A., Suberi, A., Zhou, L., Luyten, S., Reschke, M., Dong, H., Homer, R.J., Saltzman, W.M., and Iwasaki, A. (2022). Unadjuvanted intranasal spike vaccine elicits protective mucosal immunity against sarbecoviruses. Science *378*, eabo2523.

McCallum, M., De Marco, A., Lempp, F.A., Tortorici, M.A., Pinto, D., Walls, A.C., Beltramello, M., Chen, A., Liu, Z., Zatta, F., *et al.* (2021). N-terminal domain antigenic mapping reveals a site of vulnerability for SARS-CoV-2. Cell.

Olmedillas, E., Rajamanickam, R.R., Avalos, R.D., Sosa, F.A., Zandonatti, M.A.,

Harkins, S.S., Shresta, S., Hastie, K.M., and Saphire, E.O. (2023). Structure of a SARS-CoV-2 spike S2 subunit in a pre-fusion, open conformation. bioRxiv : the preprint server for biology.

Raybould, M.I.J., Kovaltsuk, A., Marks, C., and Deane, C.M. (2021). CoV-AbDab: the coronavirus antibody database. Bioinformatics *37*, 734-735.

Sesterhenn, F., Yang, C., Bonet, J., Cramer, J.T., Wen, X., Wang, Y., Chiang, C.I., Abriata, L.A., Kucharska, I., Castoro, G.*, et al.* (2020). De novo protein design enables the precise induction of RSV-neutralizing antibodies. Science *368*.

Vishweshwaraiah, Y.L., Hnath, B., Rackley, B., Wang, J., Gontu, A., Chandler, M., Afonin, K.A., Kuchipudi, S.V., Christensen, N., Yennawar, N.H., and Dokholyan, N.V. (2022). Adaptation-proof SARS-CoV-2 vaccine design. Advanced functional materials *32*.

Voss, W.N., Hou, Y.J., Johnson, N.V., Delidakis, G., Kim, J.E., Javanmardi, K., Horton, A.P., Bartzoka, F., Paresi, C.J., Tanno, Y.*, et al.* (2021). Prevalent, protective, and convergent IgG recognition of SARS-CoV-2 non-RBD spike epitopes. Science *372*, 1108-1112.

Wang, Z., Muecksch, F., Cho, A., Gaebler, C., Hoffmann, H.H., Ramos, V., Zong, S., Cipolla, M., Johnson, B., Schmidt, F.*, et al.* (2022). Analysis of memory B cells identifies conserved neutralizing epitopes on the N-terminal domain of variant SARS-Cov-2 spike proteins. Immunity *55*, 998-1012 e1018.

Xu, K., Gao, P., Liu, S., Lu, S., Lei, W., Zheng, T., Liu, X., Xie, Y., Zhao, Z., Guo, S.*, et al.* (2022). Protective prototype-Beta and Delta-Omicron chimeric RBD-dimer vaccines against SARS-CoV-2. Cell *185*, 2265-2278 e2214.

Yang, J., Liu, M.Q., Liu, L., Li, X., Xu, M., Lin, H., Li, M., Yan, H., Chen, Y.Q., and Shi, Z.L. (2023a). The protective nasal boosting of a triple-RBD subunit vaccine against SARS-CoV-2 following inactivated virus vaccination. Signal transduction and targeted therapy *8*, 151.

Yang, Y., Zhang, J., Zhang, S., Zhang, C., Shen, C., Song, S., Wang, Y., Peng, S., Gong, X., Dai, J.*, et al.* (2023b). A novel nanobody broadly neutralizes SARS-CoV-2 via induction of spike trimer dimers conformation. Exploration, 20230086.

Yuan, M., Liu, H., Wu, N.C., and Wilson, I.A. (2021). Recognition of the SARS-CoV-2 receptor binding domain by neutralizing antibodies. Biochemical and biophysical research communications *538*, 192-203.